Unsteady gaseous flows in tapered microchannels

Aubert C., Colin S., and Caen R.

Abstract-- The aim of the paper is to contribute to the modeling of unsteady slip flows in rectangular microchannels with slowly varying cross-sections.

A model is proposed for a microdiffuser submitted to sinusoidal pressure fluctuations at one of its ends. The role of the geometrical parameters is analyzed and the influence of slip at the walls is underlined. It is notably shown that the band pass of the microdiffuser is underestimated, when slip at the walls is not taken into account.

Then the model is used to test the diode effect of such a diffuser placed in a microchannel, submitted to sinusoidal pressure fluctuations at its inlet. Two layouts (A and B) are considered: the direction of the diffuser is such that section increases from inlet to outlet in layout A, and decreases in layout B. A gain is defined as the ratio of the outlet over inlet fluctuating pressure amplitudes. To characterize the transmission of pressure fluctuations, an efficiency *E* of the diode is introduced. This efficiency (defined as the ratio of the gain in layout A over the gain in layout B) is studied, as a function of the frequency. With a microdiffuser, *E* appears to be less than unity *below* a critical frequency. This denotes a diode effect reversed compared with the case of a diffuser with millimetric dimensions, for which *E* is less than unity *beyond* a critical frequency.

An analysis of these results is presented, with the purpose of better understanding the behavior of micropumps which use diffuser/nozzle-type microdiodes, and can present a peak of the mean flow at a precise frequency (typically between 1 kHz and 10 kHz), sometimes followed (for higher frequencies) by an inversion of the mean flow direction. It is suggested that the direction of the mean flow, as well as this typical frequency, may be predicted by the previous model, assuming that the mean flow results from a change in the local mean pressure. This change could be due to the increase of pressure fluctuations, notably through non-linear convective terms in the momentum equation.

Index Terms—microfluidics, slip flow, frequency behavior, micropump, fluidic diode.

I. INTRODUCTION

In the last few years, interest for valveless micropumps has noticeably increased. The use of specially designed fluidic diodes, in place of classical passive microvalves, has the advantage of limiting wear, fatigue and clogging, usually favored by mechanical moving elements with complex geometry. Following first prototypes with millimetric dimensions [1], several valveless micropumps have recently been realized. These micropumps require two or four nozzle/diffuser-type diodes, which are simply 2-D [2, 3, 4] or 3-D [5,6] converging or diverging microchannels. These diodes are placed upstream and downstream from a pump chamber, submitted to periodic pressure and volume changes induced by an excited oscillating membrane. Since flow losses are not the same in a convergent or a divergent channel, a mean flow is induced. Available experimental data point out interesting features. As an example, a peak in the pump rate vs. frequency characteristics [2,5,6] is observed. This corresponds to an optimum efficiency of the micropump, obtained for a precise value of the exciting frequency of the membrane. In some particular cases, the mean flow [5,6] can even become negative for much higher frequencies. Although simple models have been developed, they are notably limited by a simplifying assumption of quasi-static behavior. Moreover, these models are restricted to an incompressible approach, unable to treat a gas flow, especially if dimensions are such that the regime becomes rarefied. So, to come to a better understanding of how can work a valveless micropump when it pumps a gas, it is necessary to model unsteady gaseous flows through nozzle/diffuser-type diodes, taking into account rarefied effects. At the moment, there is no available tools to completely achieve this aim. Nevertheless, several analytical models of compressible flows in converging or diverging channels were published during the seventies. For example, low Reynolds effects have been studied by Manton [7], but for a steady incompressible flow. Pulsed regimes have later been considered, notably by Hall [8] for an incompressible flow, and by Caen [9] for a compressible flow, but without taking into account rarefaction effects. More recently, Dorrepaal [10] has given an analytical solution for incompressible flows in converging and diverging channels with slip at the wall, but this slip was not due to rarefaction effects. Slip flow effects due to an increase of the Knudsen number in a converging/diverging channel has been studied by Piekos and Breuer [11], but by a numerical method, using direct simulation Monte Carlo, and for a steady flow.

To complete these studies, the present paper is a contribution to the modeling of unsteady gaseous slip flows in rectangular microchannels with slowly varying cross-sections. The results of the proposed model are analyzed with the purpose of better understanding the behavior of micropumps which use nozzle/diffuser-type microdiodes.

Laboratoire de Génie Mécanique de Toulouse, INSAT,
Complexe Scientifique de Rangueil, 31077 Toulouse Cedex 04, France

II. MICRODIFFUSER AND MICRONOZZLE MODELING

In this section, a rectangular microchannel with slowly varying cross-section (fig. 1-a) is considered. It can be a diffuser (if its cross-section increases along z) or a nozzle (if this section decreases). The depth and the semi-angle of the diffuser -or nozzle- are respectively denoted by $2h$ and α. The diffuser -or nozzle- is discretized into n uniform pneumatic lines with the same length l (fig. 1-b). The cross-section of each of these elementary segments is characterized by its width $2\,b_k$ and its aspect ratio

$$a_k = \frac{h}{b_k} \tag{1}$$

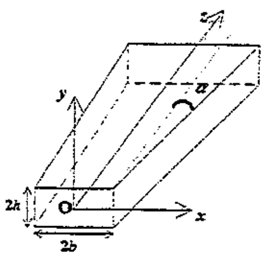

Figure 1-a

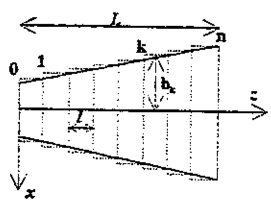

Figure 1-b

For each elementary line, the following assumptions have been made:

- the flow under consideration is assumed to be laminar and to behave as an ideal gas flow. The shear viscosity and thermal conductivity are assumed constant.
- the gas is initially at rest and then subjected to small pressure fluctuations. Each variable (pressure, density, temperature and velocity) may be written as follows: $\bar{g}(x,y,z) + g(x,y,z,t)$. The fluctuations g are supposed small compared with the mean values $\bar{g}$ for the pressure, the density and the temperature.
- the flow is considered as fully developed in each elementary line; this requires angle α to be small enough.
- the fluctuating flow is supposed parallel to the z-axis, that is, a plane wave hypothesis is made. The sole z component of velocity is denoted by w.
- the fluctuating pressure is constant within the cross-section.

Then, as a result of the previous assumptions, the fluctuating gas flow in each pneumatic line must satisfy the following continuity, momentum balance, energy conservation and state equations:

$$\frac{\partial \rho}{\partial t} + \frac{\partial(\bar{\rho}\, w)}{\partial z} = 0 \tag{2}$$

$$\frac{\partial^2 w}{\partial x^2} + \frac{\partial^2 w}{\partial y^2} - \frac{\bar{\rho}}{\mu}\frac{\partial w}{\partial t} = \frac{1}{\mu}\frac{\partial p}{\partial z} \tag{3}$$

$$\frac{\partial^2 \tau}{\partial x^2} + \frac{\partial^2 \tau}{\partial y^2} - \frac{\sigma \bar{\rho}}{\mu}\frac{\partial \tau}{\partial t} = -\frac{\sigma}{\mu C_p}\frac{\partial p}{\partial t} \tag{4}$$

$$p = r\left(\bar{\rho}\,\tau + \rho\,\bar{\tau}\right) \tag{5}$$

in which ρ, p, τ are respectively the fluctuations of density, pressure and temperature. C_p denotes the specific heat at constant pressure; $\bar{\tau}$ and $\bar{\rho}$ represent the gas temperature and density at rest; μ denotes the shear viscosity, r the gas constant and t the time variable; σ denotes the Prandtl number and is defined by:

$$\sigma = \frac{\mu C_p}{k} \tag{6}$$

where k is the coefficient of thermal conductivity.

With encountered dimensions in microsystems and under usual pressure and temperature conditions, flow is rarefied with slip and temperature jump at the walls. These conditions are represented by Maxwell-Smoluchowski first order equations.

$$w|_{y=h} = -2h\kappa K\left[\frac{\partial w}{\partial y}\right]_{y=h},\; w|_{x=b} = -2h\kappa K\left[\frac{\partial w}{\partial x}\right]_{x=b} \tag{7}$$

$$\left[\frac{\partial w}{\partial y}\right]_{y=0} = 0,\; \left[\frac{\partial w}{\partial x}\right]_{x=0} = 0 \tag{8}$$

$$\tau|_{y=h} = -\left(\frac{2-\alpha_a}{\alpha_a}\right)\frac{2\gamma}{\gamma+1}\,\frac{2hK\,\kappa_0}{\sigma}\left[\frac{\partial \tau}{\partial y}\right]_{y=h} \tag{9}$$

$$\tau|_{x=b} = -\left(\frac{2-\alpha_a}{\alpha_a}\right)\frac{2\gamma}{\gamma+1}\,\frac{2hK\,\kappa_0}{\sigma}\left[\frac{\partial \tau}{\partial x}\right]_{x=b} \tag{10}$$

$$\left[\frac{\partial \tau}{\partial x}\right]_{x=0} = 0\;,\; \left[\frac{\partial \tau}{\partial y}\right]_{y=0} = 0 \tag{11}$$

In these equations, K represents the Knudsen number defined as

$$K = \frac{\lambda}{2h} \tag{12}$$

where λ is the molecular mean free path. γ represents the ratio of the specific heats and α_a denotes the thermal accommodation coefficient. The coefficient κ is equal to $\kappa_0 \frac{2-\xi}{\xi}$ where κ_0 is a constant very nearly unity and ξ denotes Maxwell's specular reflection coefficient.

As shown in a previous paper [12], the inlet pressure and mass flow complex amplitudes can be related to the outlet pressure and mass flow complex amplitudes for a pneumatic line k, the length of which is l, the cross-sectional area S_k and the aspect ratio a_k. Assuming that the singular pressure drop which is due to the sudden enlargement is neglected with respect to the distributed pressure drop (this is justified because of the small Reynolds numbers), the flow through the diffuser is modeled as a flow through n pneumatic lines connected in series. Under sinusoidal pulsed regime, the relation between the inlet and the outlet pressure and mass flow complex amplitudes is, for a microdiffuser or a micronozzle:

$$\begin{bmatrix} p_e & m_e \end{bmatrix} = \begin{bmatrix} p_s & m_s \end{bmatrix}\prod_{k=1}^{n} A_k = \begin{bmatrix} p_s & m_s \end{bmatrix}\begin{bmatrix} B_1 & B_2 \\ B_3 & B_4 \end{bmatrix} \tag{13}$$

where subscripts e and s respectively refer to the diffuser/nozzle inlet and outlet, and

$$A_k = \begin{bmatrix} \cosh(\beta_k\, l) & \sinh(\beta_k\, l)/\eta_k \\ \eta_k \sinh(\beta_k\, l) & \cosh(\beta_k\, l) \end{bmatrix} \tag{14}$$

where $\beta_k = \sqrt{Z_k\, I_k}$ and $\eta_k = \sqrt{Z_k / I_k}$ are respectively the propagation factor and the characteristic impedance of the segment k. In these equations,

$$Z_k = \frac{2\mu}{\bar{\rho}\, S_k^{\,2}\, a_k}\left[\varphi\right]^{-1} \tag{15}$$

with

$$\varphi = \sum_{i=1}^{\infty} \frac{a_k\ \sin^2(b_i)}{b_i^{\,2}(1+2\,K\kappa \sin^2(b_i))\ (b_i^{\,2}+\mathrm{j}\,\omega_r)^{3/2}}\ \chi_i \tag{16}$$

and

$$\chi_i = \frac{\sqrt{\left(b_i^2+\mathrm{j}\,\omega_r\right)}}{a_k} + \\ - \frac{\tanh\left(\dfrac{\sqrt{b_i^{\,2}+\mathrm{j}\,\omega_r}}{a_k}\right)}{1+2\,K\kappa\sqrt{b_i^{\,2}+\mathrm{j}\,\omega_r}\ \tanh\left(\dfrac{\sqrt{b_i^{\,2}+\mathrm{j}\,\omega_r}}{a_k}\right)} \tag{17}$$

where $\mathrm{j}^2 = 1$, $\omega_r = h^2\omega\bar{\rho}/\mu$ and b_i are the solutions of

$$b_i \tan b_i = \frac{1}{2K\kappa} \tag{18}$$

Similarly,

$$I_k = \mathrm{j}\,\omega\frac{S_k\, r}{\bar{\tau}\gamma}\left[\gamma - 2\mathrm{j}\,\sigma\,\omega_r(\gamma-1)\ \psi\right] \tag{19}$$

with

$$\psi = \sum_{i=1}^{\infty} \frac{a_k\ \sin^2(c_i)}{c_i^{\,2}(1+\phi\ \sin^2(c_i))\ (c_i^{\,2}+\mathrm{j}\,\omega_r\ \sigma)^{3/2}}\ \theta_i \tag{20}$$

and

$$\theta_i = \frac{\sqrt{\left(c_i^2+\mathrm{j}\ \omega_r\ \sigma\right)}}{a_k} + \\ - \frac{\tanh\left(\dfrac{\sqrt{c_i^{\,2}+\mathrm{j}\,\omega_r\ \sigma}}{a_k}\right)}{1+\phi\sqrt{c_i^{\,2}+\mathrm{j}\,\omega_r\ \sigma}\ \tanh\left(\dfrac{\sqrt{c_i^{\,2}+\mathrm{j}\,\omega_r\ \sigma}}{a_k}\right)} \tag{21}$$

where $\phi = \left(\dfrac{2-\alpha_a}{\alpha_a}\right)\dfrac{4\gamma\ K\kappa_0}{(\gamma+1)\sigma}$ and c_i are the solutions of

$$c_i \tan c_i = \frac{1}{\phi} \tag{22}$$

As an illustration, the simple case of a diffuser element closed at its outlet by a rigid wall (fig. 6) is considered. The outlet instantaneous mass flow is thus equal to zero. So, the ratio of the outlet over inlet complex fluctuating pressure amplitudes can be obtained from equation (13) as:

$$\frac{Ps}{Pe} = \frac{1}{B_1} \tag{23}$$

As our interest lies more in the ratio of the outlet over the inlet pressure amplitudes, a gain P^* obtained from the modulus of equation (23) is defined:

$$P^* = \left|\frac{Ps}{Pe}\right| \tag{24}$$

III. Analysis

The previous model is now used to check the influence of geometrical parameters and Knudsen number on the frequency response of a micro diffuser or nozzle. As an example, theoretical results for a diffuser element are presented in this paper.
The diffuser element in question has a depth ranging from .62 µm to 10 µm. Consequently, under usual pressure and temperature conditions ($\bar{\tau} \approx 293\,K$ and $\bar{p} \approx .11$ MPa), the Knudsen numbers K are between .015 and .1. Each diffuser element is discretized into 100 uniform segments with equal lengths. Figures 2, 3, 4 and 5 respectively emphasize the role of the number of segments n, the length L, the depth $2h$ and the semi-angle α on the band pass at -3 dB for example. It is shown that whatever the case, the band pass is underestimated when slip is not taking into account.

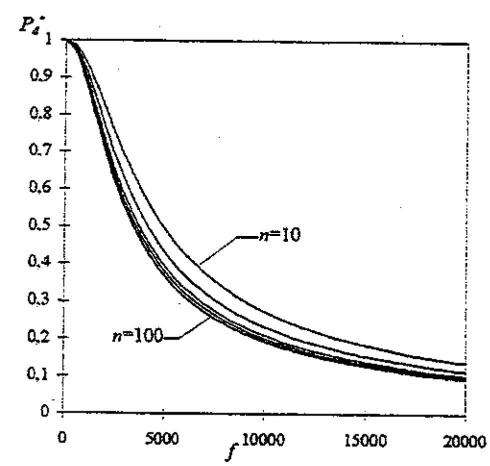

Figure 2: Influence of discretization. n=10; 20; 60; 100.

In figure 2, the microdiffuser is 6 µm in depth, 1 mm in length, the inlet is 6µm in width and the semi-angle is 3.5°. The evolution of the microdiffuser gain P_d^* is plotted for different values of the number n. As n increases, the curves converge to an asymptotic solution. For n higher than 100, the deviation to this solution can be neglected. Note that the assumption of a fully developed flow inside each elementary segment of the diffuser only involves that angle α has to remain small. Actually, the choice of number n, that is the choice of the elementary segments length l, does not seem to modify the validity of this assumption: as l decreases, the variation of the channel width also decreases, and the undeveloped effects are negligible, since they are restricted to a very small area.

Figure 3 represents the evolution of the gain P_d* as a function of the frequency for different values of the depth $2h$. The diffuser divergence semi-angle is 3.5°, the length L is 1mm, the neck width is 6 µm and the depth has a value of 1 µm and .6 µm. The increase of the diffuser inlet area obviously leads the band pass to increase. The influence of slip at the walls is pointed out, by comparing the slip model with a no-slip model (for which K=0).

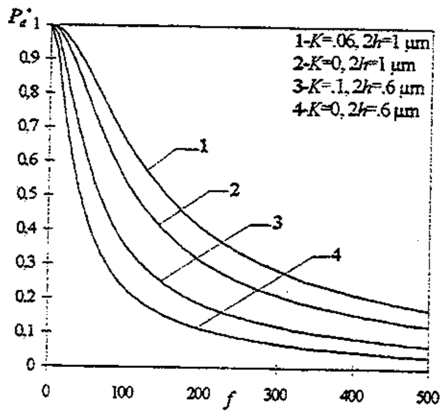

Figure 3: Influence of the microdiffuser depth $2h$.

Figure 4 represents the evolution of the ratio P_d* for different lengths L. The inlet width is 6 µm, the depth is 1µm and the semi-angle is 3.5°. The decrease of the length naturally leads the band pass to increase whether slip is taking into account or not.

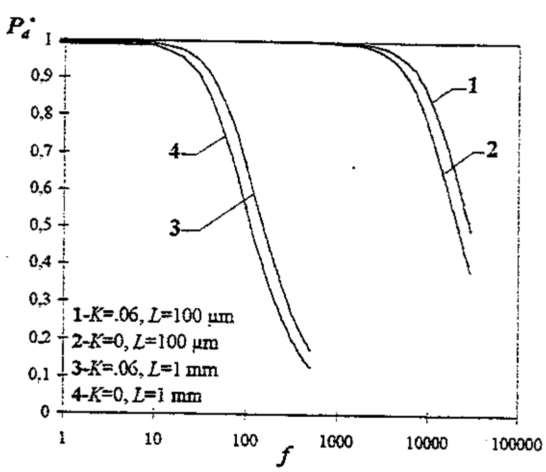

Figure 4: Influence of the microdiffuser length L.

In figure 5, the inlet area is 6 µm², the length is 1 mm and the semi-angle has a value of 2° and 5°. The outlet area increases with α, which leads to a decrease of P_d*.

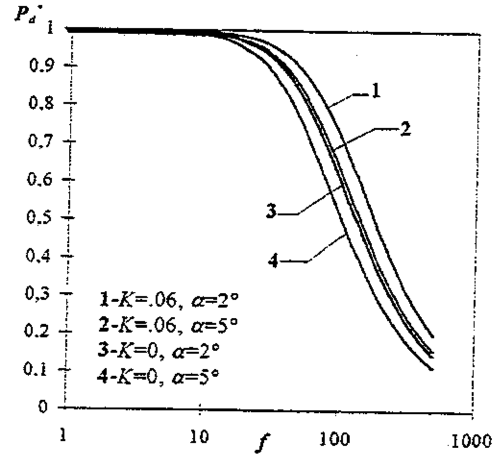

Figure 5: Influence of the microdiffuser semi-angle α.

In short, the analysis emphasizes two points. The behavior of a microdiffuser is not inherently different from the one of a sub-millimetric diffuser. But it is shown that by not taking into account slip at the walls, the band pass of the microdiffuser is underestimated.

IV. DIODE-TYPE BEHAVIOR OF THE MICRO DIFFUSER/NOZZLE

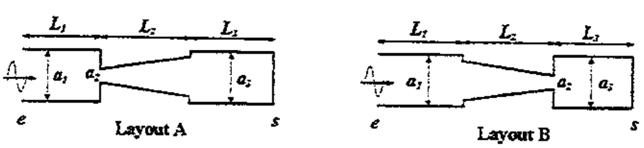

Figure 6: Layouts of a diode placed in a channel.

The model is used to test the diode effect of a micro diffuser/nozzle placed in a microchannel and submitted to sinusoidal pressure fluctuations at its inlet. Two layouts A and B are considered (fig. 6). In layout A, the tested element is a diffuser, which section increases from inlet to outlet. In layout B, the same element is used as a nozzle and its section decreases from inlet to outlet. To obtain an exploitable comparison between the two layouts, dimensions $(a_1, a_2, a_3, L_1, L_2, L_3)$ are the same in layouts A and B. The analysis of the frequency behavior for each layout shows significant differences, which is characteristic of a dynamic diode effect. So, in order to characterize the dissymmetry of the pressure fluctuations transmission, an efficiency E of the diode is introduced. This efficiency

$$E = \frac{P*_A}{P*_B} = \left|\frac{Ps}{Pe}\right|_A \Bigg/ \left|\frac{Ps}{Pe}\right|_B \qquad (25)$$

defined as the ratio of the gain in layout A over the gain in layout B, is studied as a function of the frequency. Some results are shown in figure 7, for different values of the depth $2h$, with $L_1 = L_2 = L_3 = 3\,\text{mm}$, $a_1 = a_3 = 467\,\mu\text{m}$ and $a_2 = 100\,\mu\text{m}$, which corresponds to $\alpha = 3.5°$.

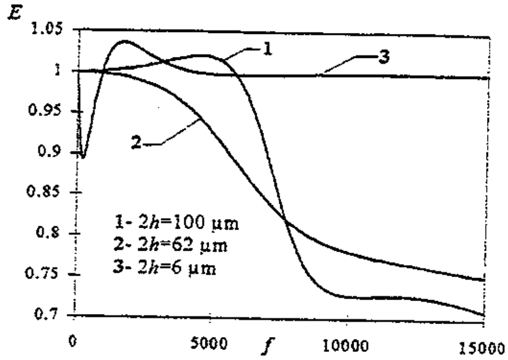

Figure 7: Diode efficiency for different values of the depth.

The main result is: with a microdiffuser ($2h = 6\,\mu m$), E appears to be less than unity *below* a critical frequency. This denotes a diode effect reversed compared with the case of a diffuser with millimetric or sub-millimetric dimensions ($2h = 100\,\mu m$ in figure 7), for which E is less than unity *beyond* a critical frequency. Note also that the influence of slip (taken into account in figure 7) is not negligible when $2h = 6\,\mu m$. However, slip has little influence on the values of characteristic frequencies (i.e. the frequencies for which E is an extremum or equal to unity).

V. About Micropumping

The question is now: to what measure does the efficiency E give useful information about the behavior of a valveless micropump with diffuser/nozzle-type diodes ? In other words, are we able to predict if, for a given pumping amplitude, there is an optimum frequency for which the mean flow of the micropump is maximum ? Is there also a possible critical frequency, beyond which an inversion of the pumping direction appears ?

We suggest that the difference of P^* evolution for a nozzle and a diffuser (expresses by the deviation of efficiency E from unity) is one of the main causes of a mean flow appearance. So, it is assumed that there is a transfer from fluctuating energy to mean energy, which results in an increase of the local mean pressure. For a given exciting frequency, due to the difference of P^* evolution, this increase is not the same at the outlet of the diffuser and at the outlet of the nozzle, placed on both sides of the pumping chamber.

In fact, the transfer from fluctuating to mean pressure is a known phenomena, which can be explained by taking into account non-linear effects, notably due to convective terms in the momentum equation. Although these non-linear terms have not been considered in the previous model - this can slightly modify the amplitude and the shape of E vs. f characteristics -, it seems that these characteristics can be qualitatively exploited.

In an attempt to validate these assumptions, simple experimental measurements have been performed, but at first on a device (fig. 8) with millimetric dimensions, for reasons of available pressure sensors dimensions.

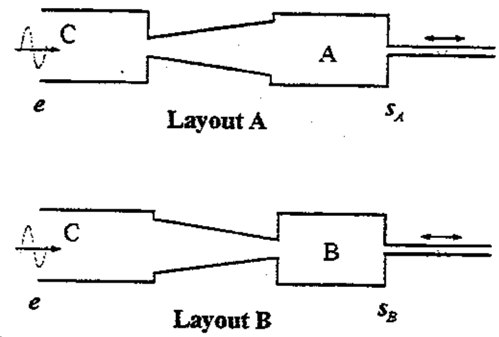

Figure 8: Schema of millimetric experimental setup.

A sinusoidal pressure fluctuation - around atmospheric pressure - is generated in chamber C. This chamber is connected to another chamber A (or B) through a diffuser (or a nozzle). Geometrical dimensions are the same in layouts A or B. A hole has been drilled at the end of both chambers A and B. Its impedance is large enough, in order not to appreciably modify the flow dynamics of the system. The fluctuating and above all the mean flows can be observed, by mean of a bubble in a capillary placed at the hole outlet. Both fluctuating and mean pressures are measured using sensors located in sections e, s_A and s_B.

The main observations are:

- for each layout, a mean flow is observed, as soon as the fluctuating pressure amplitude in section s_A (or s_B) reaches a sufficient level.
- this flow is maximum when the amplitude is maximum (which corresponds, for the millimetric device, to a resonance).
- it is noticed that this flow is correlated to an increase of the local mean pressure $\overline{P}_{s_A}$ (or $\overline{P}_{s_B}$) in section s_A (or s_B).

Since $\overline{P}_{s_A}$ and $\overline{P}_{s_B}$ have different values for a given frequency f, the flow is different in the two layouts, which can explain the behavior of a pump made of two diodes placed on both sides of a pumping chamber.

The efficiency E previously defined can be correlated with an efficiency

$$E_m = \frac{\overline{P}_{s_A} - P_a}{\overline{P}_{s_B} - P_a} \quad (26)$$

expressing the dissymmetry of the mean pressure in layouts A and B; P_a being the atmospheric pressure, which is also the mean pressure $\overline{P}_e$ in chamber C. As an example, a typical comparison between the theoretical efficiency E (fig. 9) and the experimental efficiency E_m (fig. 10) is presented. The same typical frequencies are observed, and the inversion phenomena appears for E (linked to pressure fluctuations) as well as for E_m (linked to the mean pressures).

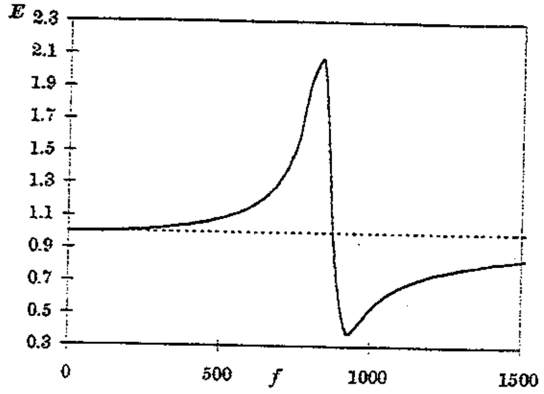

Figure 9: Theoretical efficiency E.

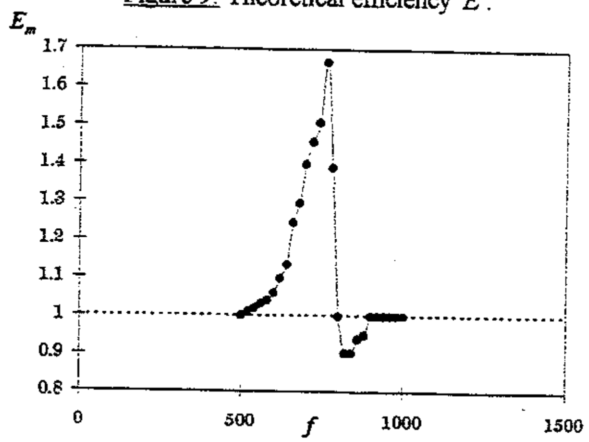

Figure 10: Experimental efficiency E_m.

VI. PERSPECTIVES

Further works will be notably focused on:

- the theoretical relation between fluctuating and mean flow, by taking into account the non-linear effects,
- systematic experimental validations, with diodes of sub-millimetric and micrometric dimensions,
- the optimization of the diodes geometry, in function of the behavior of the actuating membrane, in order to reach the best possible efficiency of the pump.

VII. REFERENCES

[1] Stemme E. and Stemme G., 1993, "A valveless diffuser/nozzle-based fluid pump", Sensors and Actuators A, 39, pp. 159-167.

[2] Olsson A., Stemme G. and Stemme E., 1995, "A valve-less planar fluid pump with two pump chambers", Sensors and Actuators A, 46-47, pp. 549-556.

[3] Olsson A., Stemme G. and Stemme E., 1996, "Diffuser-element design investigation for valve-less pumps", Sensors and Actuators A, 57, pp. 137-143.

[4] Olsson A., Enoksson P., Stemme G. and Stemme E., 1995, "Micromachined flat-walled valveless diffuser pumps", Journal of Microelectromechanical Systems, 46-47, pp. 549-556.

[5] Gerlach T., Schuenemann M. and Wurmus H., 1995, "A new micropump principle of the reciprocating type using pyramidic micro flowchannels as passive valves", Journal of Micromechanics and Microengineering, 5, N° 2, pp. 199-201.

[6] Gerlach T. and Wurmus H., 1995, "Working principle and performance of the dynamic micropump", Sensors and actuators A, 50, pp.135-140.

[7] Manton M. J., 1971, "Low Reynolds number flow in slowly varying axisymmetric tubes", Journal of Fluid Mechanics, 49, N° 3, pp. 451-459.

[8] Hall P., 1974, "Unsteady viscous flow in a pipe of slowly varying cross-section", Journal of Fluid Mechanics, 64, N° 2, pp. 209-226.

[9] Caen R., 1979, "Contribution à l'étude des écoulements instationnaires dans les circuits pneumatiques. Applications à la réponse fréquentielle d'un amplificateur fluidique analogique", Thèse de Doctorat d'Etat, INP Toulouse.

[10] Dorrepaal J. M., 1993, "Slip flow in converging and diverging channels", Journal of Engineering Mathematics, 27, pp. 343-356.

[11] Piekos E. S. and Breuer K. S., 1996, "Numerical modeling of micromechanical devices using the direct simulation Monte Carlo method", Journal of Fluid Engineering, 118, pp. 464-469.

[12] Colin S., Aubert C. and Caen R., 1998, "Unsteady gaseous flows in rectangular microchannels: frequency response of one or two pneumatic lines connected in series", European Journal of Mechanics, B/Fluids, 17, N°1, pp. 79-104.